

Generative Hierarchical Temporal Transformer for Hand Action Recognition and Motion Prediction

Yilin Wen^{1,2} Hao Pan³ Takehiko Ohkawa² Lei Yang^{4,1} Jia Pan^{1,4}
Yoichi Sato² Taku Komura¹ Wenping Wang⁴

¹The University of Hong Kong ²The University of Tokyo ³Microsoft Research Asia ⁴TransGP ⁵Texas A&M University

{ylwen, lyang, jpan, taku}@cs.hku.hk haopan@microsoft.com

{ohkawa-t, ysato}@iis.u-tokyo.ac.jp wenping@tamu.edu

Abstract

We present a novel framework that concurrently tackles hand action recognition and 3D future hand motion prediction. While previous works focus on either recognition or prediction, we propose a generative Transformer VAE architecture to jointly capture both aspects, facilitating realistic motion prediction by leveraging the short-term hand motion and long-term action consistency observed across timestamps. To ensure faithful representation of the semantic dependency and different temporal granularity of hand pose and action, our framework is decomposed into two cascaded VAE blocks. The lower pose block models short-span poses, while the upper action block models long-span action. These are connected by a mid-level feature that represents sub-second series of hand poses. Our framework is trained across multiple datasets, where pose and action blocks are trained separately to fully utilize pose-action annotations of different qualities. Evaluations show that on multiple datasets, the joint modeling of recognition and prediction improves over separate solutions, and the semantic and temporal hierarchy enables long-term pose and action modeling.

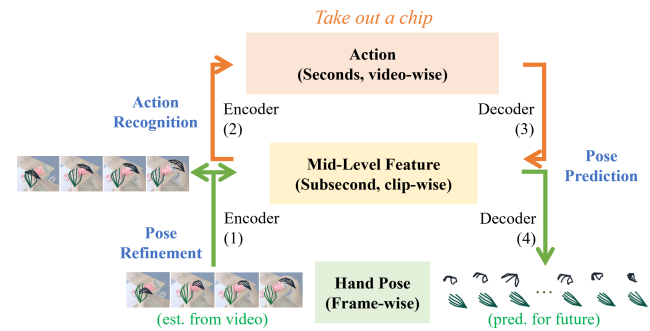


Figure 1. Jointly modeling recognition and prediction, while following the semantic dependency and temporal granularity for hand pose-action. For recognition, (1)→(2) moves up from short clips to long spans for input pose refinement and action recognition respectively. For motion prediction, two paths are available: (1)→(4) leverages short-term motion regularity, and (1)→(2)→(3)→(4) enables long-term action guided prediction.

action-conditioned motion generation, which can be used to synthesize data for recognition training. Nevertheless, the separate solutions for recognition and prediction tend to overfit to specific data distributions, lacking robust performance generalization (Sec. 4.3).

We present a framework with generative Transformer VAE architecture to jointly model both action recognition and motion prediction. The joint modeling enables exploiting the temporal regularity of short-term hand motion and long-term action shared through the observation (*e.g.* hand poses to reach into the can, indicating the action of taking out a chip) and future timestamps (*e.g.* predicted poses to grab and pull out a chip, thus completing the action, see Fig. 1). Therefore, the model can address various tasks including input pose refinement, action recognition, and future motion prediction. Additionally, it can enhance the performance on these tasks compared to individual models (Sec. 4.3). Specifically, the transformer encoder is responsible for producing outputs for recognition, while the

1. Introduction

Understanding dynamic hand poses and actions is a fundamental task for human-robot interaction and VR/AR applications. While there is tremendous progress in recognizing action and predicting future hand motion as a sequence of frame-wise poses, most of the literature tackle only either the recognition [13, 43, 52, 53] or prediction [2, 25, 26] task. On the other hand, recent works demonstrate the benefits of bridging recognition and prediction. For example, [39, 44] learn motion priors through future pose prediction, and apply them to refining pose estimated in videos. Other works [28, 36, 37, 48] learn generative models of

decoder is responsible for prediction. The VAE latent space connects the two by extracting regular motion and action priors, which are shared between the observed sequences and future motion.

Moreover, when it comes to pose-action modeling, extensive previous works [8, 14, 25, 28, 36, 37, 47, 48, 52, 53] demonstrate the importance of capturing the semantic dependency of hand sequences in different temporal granularities, *i.e.* the instantaneous pose and the action over seconds. For example, [8, 47, 52, 53] first locate the hand motion (*e.g.* hand poses to reach into the can, grab a chip, and pull out the chip) from the observed video, and use it to recognize the performed action (*e.g.* take out a chip). [52] further proposes *Hierarchical Temporal Transformer* to model the semantic dependency and temporal granularity of pose and action with two cascaded encoders respectively working on short and long time spans, for effective hand pose estimation and action recognition. On the generation side, [14, 28, 36, 37, 48] generate more realistic motion by conditioning on action.

Inspired by [52], in addition to jointly modeling both recognition and prediction, we faithfully respect the semantic dependency and temporal granularity of hand pose-action, which improves over flattened models (Sec. 4.4). Our framework, named *Generative Hierarchical Temporal Transformer* (G-HTT), consists of two cascaded blocks that have the same generative transformer VAE structure but focus on different semantic and temporal granularities: the lower pose block models hand poses over short time spans, and the upper action block models action over long time spans. Meanwhile, the two blocks are bridged by a middle-level representation, *i.e.* the pose block VAE latent code, which encodes clip-wise motion over a subsecond span (Fig. 1). The hierarchy further brings training flexibility, as we can train the blocks separately, which not only reduces training computational demands but also allows for using training data with pose-action annotations of different qualities (Secs. 3.4 and 4.5).

We train and evaluate the framework across different datasets of two-hand interactions, including H2O [22] for daily activities, Assembly101 [42] and Assembly-Hands [35] for (dis-)assembling take-part toys. At test time, given a 3D hand pose sequence (*e.g.* per-frame estimations from the observed RGB video), we first refine it by leveraging the short-term hand motion regularity, (Fig. 1, (1)). Next, we aggregate the clip-wise motions for action recognition (Fig. 1, (1)→(2)). Finally, we decode the observed action and motions into a sequence of future middle-level features for motion prediction (Fig. 1, (1)→(2)→(3)→(4)). Evaluation results across datasets show that our framework can solve recognition problems from various camera views, and produce plausible future hand poses over time. The contribution of this paper can be summarized as follows:

- A joint modeling of hand action recognition and motion prediction with generative transformer VAEs, which exploits the temporal regularity of motion and action shared between the observed and future timestamps, thus contributing to robust performance generalization,
- A specialized architecture composed of two generative blocks that model the semantic dependency and temporal granularity of pose-action, thus improving performance and training flexibility, and
- A comprehensive evaluation of the system on tasks such as 3D hand pose refinement, action recognition, and 3D motion prediction, validating the performance and design of our framework.

2. Related Works

Action recognition and 3D Hand pose estimation Massive literature addresses recognition from the visual observation, with tasks at different semantic levels. For example, a series of works aim to recover the 3D hand skeleton or mesh from the visual input, where the spatial correlation within a single-frame is well exploited [19, 23, 33, 46, 54, 58], and the motion cue along the temporal dimension is further leveraged for improved robustness under occlusion and truncation [3, 10, 15, 16, 34, 51]. Meanwhile, [5, 11–13, 43] focus on a higher semantic level, where they extract the spatial-temporal feature from the input frames to recognize the semantic hand or body action.

Moreover, many notice and exploit the benefits of modeling the semantic dependency between hand pose and action, since intuitively action is defined by the pattern of hand motion (*i.e.* verb) and object in manipulation (*i.e.* noun). For example, [8, 24, 31, 45, 47, 52, 53] leverage the hand pose features for action recognition; while [53] further refers to the action feature for pose refinement. Furthermore, a recent work [52] demonstrates the benefit of exploiting temporal cue by respecting the temporal granularity, and proposes a framework with two cascaded blocks to respectively work on short- and long- term spans and output per-frame 3D hand pose and video action. The hierarchical structure of our framework is inspired by [52], but we have extended it to model prediction tasks, which not only covers more tasks but also enhances recognition performance (Sec. 4.3).

3D Hand and human motion prediction Previous works predict the 2D or 3D trajectory of hand roots [2, 25, 26, 29] or skeleton [7] from observed hand motion, with more recent works building on powerful generative deep neural networks to capture the distributions of future sequences [1, 4, 20, 28, 30, 32, 49, 55, 56]. In motion prediction, the modeling of semantic dependency also demonstrates its benefits. On one hand, [9, 25] leverage the predicted hand trajectory and its interaction with object for improved action anticipation. On the other hand, recent works also generate more realistic pose sequences by taking the past

motion together with a specified action as condition, based on cVAEs [4, 32], GPT-like models [20, 28, 56] and diffusion models [49]. Our work builds a hierarchical structure for motion prediction, where consistency in both short-term motion and long-term action is explicitly ensured through the cascade of generative Transformer VAEs (Sec. 4.4). In addition, we learn prediction and recognition simultaneously, which improves both tasks by exploiting the shared temporal regularity (Sec. 4.3).

Bridging recognition and prediction Previous studies have shown enhanced effectiveness by bridging recognition and prediction on hand (or body) poses. For example, [39, 44] build on cVAEs to model a latent space depicting the pose transition along the temporal dimension, by learning the next frame pose prediction; the learned latent space is then leveraged as a strong regulation in optimization-based refinement of estimated pose sequences. [50] models a manifold of plausible human poses based on neural distance fields; compared with Gaussian latents, the learned manifold facilitates more accurate optimization of pose refinement and improves diversity for pose generation. Rather than relying on optimization, our framework directly addresses both recognition and prediction.

Building on advances of generative models, recent works [28, 36, 37, 48, 49] learn text-guided motion generation models, where the text guidance is in the form of prescribed actions; the generated sequences can then be used for training recognition tasks. For example, PoseGPT [28] first quantizes short motion clips into latent codes by training a VQ-VAE, and then constructs a GPT-like autoregressive model for motion generation, which learns on sequences of action and latent motion tokens. Compared with these generative models, our framework enables both pose-induced action recognition and action guided pose generation, and captures the critical semantic hierarchy between short-term pose and long-term action.

3. Methods

The core framework, namely *Generative Hierarchical Temporal Transformer* (G-HTT, Fig. 2), takes as input the object in manipulation and the observed pose sequence of T frames for two interacting hands (Sec. 3.1), where the hand motion and object feature respectively depict the *verb* and *noun* of the action being performed (e.g. take out a chip). G-HTT then jointly models both recognition and prediction, while following the semantic-temporal hierarchy of pose-action that captures their dependency and different temporal granularities (Sec. 3.2). In the test stage, we apply G-HTT to recognition tasks of input pose refinement and action recognition, and diverse hand motion prediction for future timestamps (Sec. 3.3). Important implementation details are given in Sec. 3.4, and a table of notations is provided in the supplementary for reference.

3.1. 3D Hand Motion Representation

Given a sequence depicting two interacting hands, we construct the 3D hand representation for each frame as $\mathbf{H} = (p^L, p^R, v^L, v^R, r)$, where $p^L, p^R \in \mathbb{R}^{3N}$ are the 3D coordinates for N joints of each hand aligned to a predefined template [40], $v^L, v^R \in \mathbb{R}^9$ are the relative rigid palm transformations compared with the previous frame, and $r \in \mathbb{R}^9$ are the relative rigid palm transformation between two hands in the current frame. We denote the rigid transformation v^L, v^R, r by concatenating the 6D continuous representation of rotation [57] and 3D translation. More details of \mathbf{H} encoding are given in the supplementary.

3.2. Joint Modeling of Recognition and Prediction with Semantic-Temporal Hierarchy

G-HTT consists of two cascaded blocks, namely the short-term pose block \mathbf{P} and the long-term action block \mathbf{A} , to jointly model recognition and prediction while following the hierarchy of temporal and semantic granularity for pose-action. Both \mathbf{P} and \mathbf{A} have the same VAE structure, with their encoders and decoders respectively output for recognition and future motion prediction, but they model different semantic levels and time spans (Fig. 2).

To bridge the pose and action blocks in the semantic-temporal hierarchy, we explicitly introduce a mid-level feature \mathbf{m} , which compresses the hand poses within a sub-second time span. \mathbf{P} and \mathbf{A} then respectively model the mappings between pose *vs.* mid-level, and mid-level *vs.* action. As the two blocks are cascaded, the different semantic levels can refer to each other for globally consistent recognition and prediction (Sec. 3.3). Moreover, our design enables a flexible training scenario, where \mathbf{P} and \mathbf{A} can be decoupled and trained separately based on their respective supervision signals and training data (Sec. 3.4).

P-Block takes a subsecond time span of $t (t < T)$ consecutive frames to model the relationship between per-frame hand pose and mid-level feature \mathbf{m}^P , without explicitly leveraging the action information. The mid-level \mathbf{m}^P is learned to be the latent bottleneck of \mathbf{P} , which encodes the input t consecutive frames of hand poses $\tilde{\mathbf{H}}_{1:t}$ via \mathbf{E}^P , and is decoded to hand motion $\mathbf{H}_{t+1:2t}$ of the future t frames by \mathbf{D}^P . Meanwhile, similar to [52], the observed $\tilde{\mathbf{H}}_{1:t}$ can be refined by \mathbf{E}^P leveraging short-term temporal regularity.

In detail, \mathbf{E}^P takes as input a sequence of $t + 2$ tokens $(\tilde{\mu}^P, \tilde{\Sigma}^P, \tilde{\gamma}_1, \dots, \tilde{\gamma}_t)$, where $\tilde{\gamma}_i \in \mathbb{R}^d$ encodes the per-frame hand pose $\tilde{\mathbf{H}}_i$, and $\tilde{\mu}^P, \tilde{\Sigma}^P \in \mathbb{R}^d$ are trainable tokens for parameterizing the distribution of \mathbf{m}^P by aggregating over $\tilde{\mathbf{H}}_{1:t}$, similar to [36, 37]. Denoting the output sequence of \mathbf{E}^P as $(\mu^P, \Sigma^P, \gamma_1, \dots, \gamma_t)$, we sample \mathbf{m}^P with re-parameterization [21] from the normal distribution $N(\mu^P, \Sigma^P)$, and obtain $\mathbf{H}_i = \text{MLP}_1(\gamma_i)$ as the refined per-frame hand poses for $i \in [1, t]$.

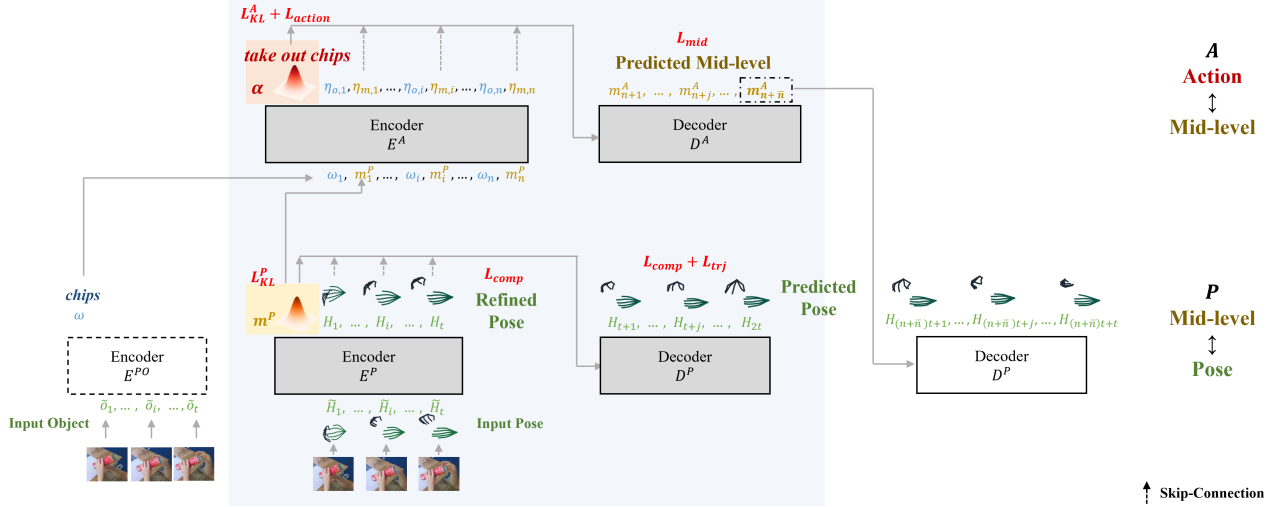


Figure 2. Overall of our framework. The cascaded **P** and **A** (denoted in the blue shadow) of G-HTT jointly model recognition and prediction, by faithfully respecting the semantic dependency and temporal granularity among pose, mid-level and action (Sec. 3.2). The two \mathbf{D}^P in the figure are identical, but decode either \mathbf{m}^P (gray) or \mathbf{m}^A (white) for motion prediction.

\mathbf{D}^P predicts the hand pose for the following t frames in a parallel manner. The mid-level \mathbf{m}^P , and $\gamma_{1:t}$ optionally as skip-connections, are referred by \mathbf{D}^P through cross-attention. As a parallel transformer decoder, the query input of \mathbf{D}^P are the sinusoidal position encoding of t tokens, and the output t tokens are mapped by MLP_1 to the future hand motion $\mathbf{H}_{t+1:2t}$.

Denoting the corresponding GT motion as $\bar{\mathbf{H}}_{1:2t}$, \mathbf{P} is trained by a loss function consisting of three parts:

- The hand component loss to compare the refined and predicted motion with GT:

$$L_{comp} = \frac{1}{2t} \sum_{i=1}^{2t} \|\bar{\mathbf{H}}_i - \mathbf{H}_i\|_1 \quad (1)$$

- The root frame trajectory loss for the predicted part:

$$L_{trj} = \frac{1}{t} \sum_{i=t+1}^{2t} (\|\bar{s}_i^L - s_i^L\|_1 + \|\bar{s}_i^R - s_i^R\|_1) \quad (2)$$

where $s_i^L, s_i^R \in \mathbb{R}^9$ are computed by accumulating v^L, v^R of $\mathbf{H}_{t+1:i}$ as

$$s_i^L = v_i^L \circ v_{i-1}^L \circ \dots \circ v_{t+1}^L, \quad s_i^R = v_i^R \circ v_{i-1}^R \circ \dots \circ v_{t+1}^R \quad (3)$$

with \circ denoting composition of rigid transformation. \bar{s}_i^L, \bar{s}_i^R denote the GT counterpart.

- The KL-loss L_{KL}^P for the regularity of \mathbf{m}^P , as the KL-divergence between $N(\mu^P, \Sigma^P)$ and the standard normal distribution.

The overall loss for \mathbf{P} sums them up: $L_P = \lambda_1 L_{comp} + \lambda_2 L_{trj} + \lambda_3 L_{KL}^P$.

A-Block models the relationship between the mid-level feature and action: it exploits the long-term time span to aggregate the sequence of mid-level features \mathbf{m}^P from the whole observation, and predicts a sequence of mid-level

features \mathbf{m}^A for future timestamps, which are further expanded by \mathbf{D}^P into concrete motion. In addition to variational auto-encoding, **A** has its latent bottleneck feature also aligned with text embeddings of the action taxonomy, to enable action recognition of the observation and action controlled prediction.

The encoder \mathbf{E}^A takes the sequence of mid-level $\mathbf{m}_{1:n}^P$ ($n = \lceil T/t \rceil$) and clip-wise object feature $\omega_{1:n}$ as input, to derive action from hand motion and object feature across the observation. In detail, we denote its input as $(\tilde{\mu}^A, \tilde{\Sigma}^A, \mathbf{m}_1^P + \phi_1, \omega_1 + \phi_1, \dots, \mathbf{m}_n^P + \phi_n, \omega_n + \phi_n)$, where $\tilde{\mu}^A, \tilde{\Sigma}^A \in \mathbb{R}^d$ are trainable tokens. For each clip $i \in [1, n]$, \mathbf{m}_i^P is the μ^P from \mathbf{E}^P ; ω_i is aggregated by an extra individual \mathbf{E}^{PO} from the per-frame object features (Sec. 3.4), and is comparable to the CLIP [6, 38, 41] feature of object name; ϕ_i is the sinusoidal phase encoding denoting the number of clips since the beginning of the performed action. Given the \mathbf{E}^A output $(\mu^A, \Sigma^A, \eta_{m,1}, \eta_{o,1}, \dots, \eta_{m,n}, \eta_{o,n})$, the bottleneck latent feature α is then re-parameterized by $N(\mu^A, \Sigma^A)$.

We inject α into decoder to enable action controlled generation. Specifically, the parallel decoder \mathbf{D}^A takes α for cross-attention, with $\eta_{m,1:n}$ optionally included as skip-connections for enhanced continuity. \mathbf{D}^A takes the phase embeddings $\phi_{n+1:n+\bar{n}}$ as input, and outputs $\mathbf{m}_{n+1:n+\bar{n}}^A$ depicting the mid-level features of the future \bar{n} consecutive clips. The predicted \mathbf{m}^A can then be further expanded into concrete poses through \mathbf{D}^P , completing the cycle of long-term observation for long-term prediction, with consistency in both global action and local poses (Sec. 3.3, P.b).

To train **A**, besides the KL-loss L_{KL}^A , we constrain α to match the embedding of action taxonomy $\mathcal{A} = \{a = \text{FC}_1(\bar{\alpha}) \in \mathbb{R}^d\}$, where $\bar{\alpha}$ are CLIP text embeddings [6, 38, 41] for action labels in the taxonomy of size N_A . The action

recognition loss is:

$$L_{action} = \sum_{i=1}^{N_A} w_i (||\alpha - a_i||_1 - \log \Pr(a_i|\alpha)) \quad (4)$$

which penalizes the differences of action features by both l_1 -norm and contrastive similarity. Here, w_i is 1 for the GT action and 0 otherwise, and

$$\Pr(a_i|\alpha) = \frac{\exp(\hat{\alpha} \cdot \hat{a}_i/\tau)}{\sum_{j=1}^{N_A} \exp(\hat{\alpha} \cdot \hat{a}_j/\tau)} \quad (5)$$

measures the probabilistic similarity of predicted and GT labels among candidates from taxonomy. $\hat{z} = z/||z||$ denotes the normalized unit vector, and $\tau = 0.07$ is the temperature of contrastive similarity. When testing, we perform action recognition by searching closest labels to μ^A .

For future motion supervision, instead of expanding down to concrete hand poses, we directly compare mid-level features for efficiency. In particular, $\mathbf{m}_{n+1:n+\bar{n}}^A$ are compared with pre-computed $\bar{\mathbf{m}}_{n+1:n+\bar{n}}^P$, where $\bar{\mathbf{m}}_j^P = \mu_j^P$ encodes the poses $\bar{\mathbf{H}}_{T+(j-1)t+1:T+jt}$ of the future j -th clip via \mathbf{E}^P . Therefore, the motion prediction loss is

$$L_{mid} = \sum_{j=n+1}^{n+\bar{n}} ||\mathbf{m}_j^A - \bar{\mathbf{m}}_j^P||_1 \quad (6)$$

To summarize, the overall loss of \mathbf{A} is $L_A = \lambda_4 L_{mid} + \lambda_5 L_{action} + \lambda_6 L_{KL}$.

3.3. Network Flow for Tasks

The framework addresses diverse tasks of recognition (including pose refinement and action recognition) and prediction by going through different paths within the network.

Recognition Recognition tasks are performed through the encoders. Specifically, \mathbf{E}^P refines the input per-frame estimated hand pose by referring to the motion regularity over a subsecond clip of t frames, followed by \mathbf{E}^A to output μ^A for action recognition over the entire T input frames.

Prediction Prediction of future hand motion is fulfilled by the decoders. Given observed hand motion $\bar{\mathbf{H}}_{1:T}$, G-HTT provides two ways for the prediction of diverse and realistic hand motions (Fig. 1):

(P.a) **(1)→(4)**. It generates locally consistent motions using only \mathbf{P} . It takes the last t observed frames $\bar{\mathbf{H}}_{T-t+1:T}$ as input, and predicts motion of the following clip $\bar{\mathbf{H}}_{T+1:T+t}$ by sampling from $N(\mu^P, \Sigma^P)$ for \mathbf{D}^P decoding. The output motion can then be autoregressively fed back to \mathbf{P} as input for longer prediction.

(P.b) **(1)→(2)→(3)→(4)**. For more realistic long-term prediction with action guidance, we move up the hierarchy to leverage \mathbf{A} and predict $\mathbf{m}_{n+1:n+\bar{n}}^A$, with diversity coming from sampling from $N(\mu^A, \Sigma^A)$. $\mathbf{m}_{n+1:n+\bar{n}}^A$ are further decoded by \mathbf{D}^P into concrete poses $\bar{\mathbf{H}}_{T+t+1:T+(\bar{n}+1)t}$.

We compare the two paths for motion prediction empirically in Sec. 4.4, and use P.b by default for long-term prediction in other experiments.

3.4. Implementation Details

\mathbf{P} , \mathbf{A} are trained across different datasets separately. To deploy G-HTT for practical RGB video processing, we leverage an external image-based hand object estimator \mathbf{F} and a sequence-based object aggregator \mathbf{E}^{PO} , to provide the input for G-HTT. The external modules can be trained independently or obtained from off-the-shelf models.

G-HTT details We set $t = 16$ and allow T to have a maximum value of 256 at 30 fps. Both \mathbf{P} and \mathbf{A} have 9 layers for the encoders and decoders, with a token dimension of $d = 512$. We train a single network across datasets with different pose and action annotation qualities for enhanced capability (Sec. 4.5).

We first train \mathbf{P} on all available pose sequences, regardless of the availability and transition of action labels, thanks to the decoupling of action and \mathbf{P} . We augment the input motion $\bar{\mathbf{H}}$ with random noise, making \mathbf{P} capable to cope with noisy per-frame estimation in the recognition stage. Then, we fix the pre-trained \mathbf{P} and train \mathbf{A} , whose training data assumes the same action shared between the observation and prediction. We derive the mid-level $\bar{\mathbf{m}}^P$ from the pose annotations with \mathbf{E}^P , randomly divide the training sequence into observed and predicted parts, and correspondingly assign $\bar{\mathbf{m}}^P$ as the input of \mathbf{E}^A or supervision signal of \mathbf{D}^A . For the input of \mathbf{E}^A , we augment the mid-level features with random Gaussian noise, and refer to the noun of GT action for the clip-wise object feature ω .

We use AdamW [27] optimizer with a learning rate of 10^{-4} and weight decay of 0.01 for both \mathbf{P} and \mathbf{A} , using a batch size of 256. We respectively train \mathbf{P} and \mathbf{A} with 80 and 200 epochs, with loss weights as $\lambda_1, \lambda_2 = 1, \lambda_3 = 10^{-5}$, and $\lambda_4 = 1, \lambda_5 = 0.1, \lambda_6 = 10^{-5}$. Other design and training details are illustrated in the supplementary.

Image-based estimator \mathbf{F} takes an image as input, and outputs for the image its hand pose, along with the object feature $\bar{\mathbf{o}}$ that is comparable with CLIP [6, 38, 41] feature of object in manipulation. For experiments, we implement \mathbf{F} as a ResNet-18 [17] backbone followed by heads regressing the hand pose and object feature. We provide more details in the supplementary.

Clip-wise object detector \mathbf{E}^{PO} extracts ω as the clip-wise object representation aggregated from per-frame object features $\bar{\mathbf{o}}$ of t consecutive frames. The clip-wise ω is then fed into \mathbf{E}^A to provide a consistent object information for action recognition (Sec. 3.2). We implement \mathbf{E}^{PO} by 2 transformer encoder layers, which is trained based on \mathbf{F} ; details are explained in the supplementary.

4. Experiments

4.1. Datasets

To demonstrate the versatility of our framework, we use three large-scale hand action datasets [22, 35, 42], covering highly diverse motions and actions, for training and testing. Across all datasets, we consider $N = 20$ joints annotated by [22], leaving the carpometacarpal joint of the thumb out as its annotation is unavailable in [42]. We train **P** on untrimmed sequences that could contain multiple action annotations, because the short-span hand motion is independent of action, and train **A** on trimmed sequences with clean and complete action annotations. For evaluation of both pose and action, we use trimmed sequences with clean action labels.

H2O [22] records four subjects performing 36 indoor daily activities, in four fixed and one egocentric camera viewpoints. We evaluate on both the validation and test splits, the latter having subjects unseen in training.

Assembly101 [42] and **AssemblyHands** [35] Assembly101 [42] contains procedures of people assembling and disassembling toy vehicles, with pose labels computed automatically by UmeTrack [16]. AssemblyHands [35] further improves the pose annotation quality for a subset of Assembly101 sequences.

We follow the splits of Assembly101 for training and testing, using actions of its fine-grained taxonomy with 1380 different labels. We conduct evaluations on sequences that have more reliable pose annotations from AssemblyHands, and consider six fixed camera views that have no severe hand occlusions (details in supplementary). We focus evaluation on the validation split, as it contains accessible object labels for action recognition and motion prediction (Secs. 4.3 and 4.4), which the test split lacks.

4.2. Setup and Metrics

Recognition We take a whole video sequence depicting the process of an action as input. For evaluation of pose estimation, we use metrics of **MPJPE-RA** (Mean Per Joint Position Error-Root Aligned) and **MPJPE-PA** (Procrustes analysis of MPJPE). To deal with the ambiguity of different hand scales, we align estimation and GT by equalizing the average length of palm bones. For action recognition, we report the top-1 classification accuracy (**Action Acc.**).

Prediction We divide each action video into segments of 16 frames. Given each segment, we use its pose and object annotation as the input observation, and predict the rest sequence until reaching the end of action or the maximum duration of 96 frames. We generate 20 random samples from $N(\mu, 5\Sigma)$ as a trade-off between accuracy and diversity (Secs. 4.3 and 4.4). For evaluation of generative results,

			Resnet-18(F)	HTT [52]	Ours
H2O Test [22]	cam0*	MPJPE-RA↓	27.0,25.6	26.9,24.1	26.5,25.3
		MPJPE-PA↓	7.8,10.6	7.3,10.4	7.4,10.3
		Action Acc.↑	-	85.12	59.92
	cam2	MPJPE-RA↓	19.2,24.8	20.1,25.4	18.9,24.5
		MPJPE-PA↓	6.9,10.6	7.4,11.0	6.6,10.3
		Action Acc.↑	-	73.55	68.18
	cam4	MPJPE-RA↓	18.4,21.4	101.2,137.8	17.9,21.0
		MPJPE-PA↓	6.8,9.4	28.5,33.8	6.4,9.1
		Action Acc.↑	-	2.89	57.85
Assembly Hands Val [35]	v1	MPJPE-RA↓	35.4,22.7	55.6,39.0	35.1,22.4
		MPJPE-PA↓	12.0,10.8	17.2,14.2	11.7,10.4
		Action Acc.↑	-	16.55	36.01
	v3*	MPJPE-RA↓	27.5,27.2	26.7,27.3	27.3,26.9
		MPJPE-PA↓	12.2,12.0	12.3,12.1	11.9,11.7
		Action Acc.↑	-	39.42	34.79
	v8	MPJPE-RA↓	26.1,30.4	91.3,88.5	25.9,30.0
		MPJPE-PA↓	11.8,12.3	24.2,27.3	11.5,11.8
		Action Acc.↑	-	9.98	36.74

Table 1. Pose estimation and action recognition results on H2O [22] and AssemblyHands [35]. For hand pose estimation we report MPJPE-RA/-PA in *mm* for (left,right) hand respectively, where * denotes training views leveraged for HTT [52]. Please refer to the supplementary for complete results on all camera views, and comparison on the H2O-Val.

we mainly use the widely adopted **FID** (Fréchet Inception Distance) [18] to assess quality, which computes the distributional distance of features between generated and GT motion sequences. The features are obtained from the last layer of a pre-trained transformer-based action recognition network, and the GT sequences are from the evaluation split unseen in training. Smaller FID means more faithful generation. In addition, to explicitly measure generation diversity, we report **APD** (Average Pairwise Diversity) [55] that computes the average distance between all pairs of 20 generated samples. Larger APD means more diverse generation. More details about the setup and metrics are given in the supplementary.

4.3. Joint Modeling of Recognition and Prediction

We first demonstrate the enhanced capability because of our joint modeling of recognition and prediction, by respectively comparing with state-of-the-art solutions for either recognition (*i.e.* HTT [52]) or prediction (*i.e.* PoseGPT [28]). More implementation details for the baselines are given in the supplementary.

Recognition The most relevant baseline is HTT [52], which also models the semantic-temporal hierarchy but focuses only on recognition. Based on the pre-trained image-based estimator **F** used by ours for fair comparison (Sec. 3.4), we train HTT on two camera views of H2O (*cam0,1*) and one view (*v3*) of AssemblyHands, where we concatenate image feature with the estimated hand pose and object from **F** as the per-frame input of HTT. We also take the initial pose estimation of **F** as a reference for comparison. Moreover, to obtain the object input for both methods, on H2O we leverage the network estimation, while on As-

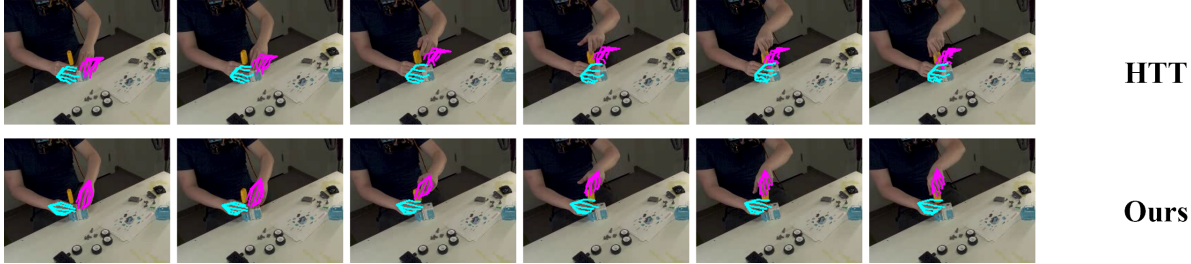


Figure 3. Qualitative comparison of pose estimation for HTT [52] and our G-HTT, on camera view v_1 of Assembly datasets [35, 42]. More cases on H2O and AssemblyHands datasets are provided in the supplementary.

semblyHands we use the GT labels, where it is very challenging to recognize objects reliably due to cluttered scenes and frequent occlusions (Fig. 3).

As shown in Tab. 1 and Fig. 3, G-HTT demonstrates robust accuracy on various camera views, for refining the local pose and action recognition, even though G-HTT is never trained on \mathbf{F} . In comparison, although HTT fits better on views that are trained on or close to trained ones (*e.g.*, *cam2* of H2O), its performance significantly degrades on the other views, even worse than its input obtained from \mathbf{F} . The results show that our simultaneous modeling of both recognition and prediction enhances generalization by learning regular motion priors across tasks. In contrast, a recognition-only network is more likely to overfit to particular data distributions.

Prediction We take PoseGPT [28], a state-of-the-art model for motion prediction with *prescribed* action, as a baseline for performance evaluation. While the original PoseGPT trains on body motion, we retrain PoseGPT with its official code by combining the three hand pose-action datasets of Assembly101 [42], AssemblyHands [35] and H2O [22] as we do. We evaluate on action sequences longer than 1 sec to better show the differences of prediction.

As reported in Tab. 2, G-HTT shows significantly better FID on the H2O-test split of unseen subjects and on AssemblyHands; meanwhile, the two methods have comparable accuracy on the H2O-val split of trained subjects. These results show our better generation quality across actions and datasets. Visually from Fig. 4, while PoseGPT suffers from lacking regularity for predicted motion, our prediction shows globally consistent action.

We attribute the differences to two factors: our joint learning of both recognition and prediction, and our hierarchical model for pose and action. In contrast to action-conditioned generation alone, by modeling both recognition and prediction our framework learns strong motion-action regularities across datasets covering highly diverse hand actions, as shown by the consistent high quality across three datasets (Tab. 2). Moreover, different from the vector quantization of PoseGPT for clip-wise motion, our mid-level representation originates from \mathbf{P} , where \mathbf{P} models not only

		Pose-GPT [28]	Ours (P.b, w/ \mathbf{P}, \mathbf{A})
Inputs with GT		motion, action	motion, object
H2O-Val	FID↓	5.19	5.32
	APD↑	32.3,43.1	22.1,25.7
H2O-Test	FID↓	11.70	8.19
	APD↑	24.1,48.6	20.1,33.9
AssemblyHands	FID↓	16.07	5.04
	APD↑	25.3, 33.0	28.1,32.8

Table 2. Comparison with PoseGPT [28] for motion prediction, on action sequences that are longer than 1 sec. APD in *mm* for (left,right) hand respectively.

		Ours(P.a, w/ \mathbf{P})	Ours (P.b, w/ \mathbf{P}, \mathbf{A})
H2O-Val	FID↓	8.18	6.59
	APD↑	40.7,48.3	29.7,33.3
H2O-Test	FID↓	12.78	10.88
	APD↑	36.7,52.5	26.2,48.3
AssemblyHands	FID↓	8.20	6.84
	APD↑	40.8,51.1	34.8,42.3

Table 3. Comparison of long-term motion prediction decoded from \mathbf{m}^P (P.a) and \mathbf{m}^A (P.b), on action sequences that are longer than 2 sec. APD in *mm* for (left,right) hands.

the observed motion but also prediction, enabling global action-guided motion generation that preserves local motion continuity (see also Sec. 4.4).

4.4. Modeling Semantic-Temporal Hierarchy

In this section, we examine the effects of modeling the semantic-temporal hierarchy. As HTT [52] has well demonstrated the benefits of leveraging this hierarchy in recognition tasks, here we mainly examine its benefits for motion prediction, especially on sequences longer than 2 secs where global action is more apparent.

Action for prediction We first compare the long-term prediction decoded from \mathbf{m}^P and \mathbf{m}^A , *i.e.*, the two strategies P.a, P.b described in Sec. 3.3, to examine the effectiveness of involving \mathbf{A} for long-term prediction.

As shown in Tab. 3 and Fig. 4, generations from \mathbf{m}^A are more realistic and plausible, with lower FID and more consistent global motion. In contrast, results of P.a show larger diversity due to its short-term modeling, but lack fidelity or regularity for long-term motion. Overall, the comparison shows the importance of action modeling in generating faithful and action-guided motions.

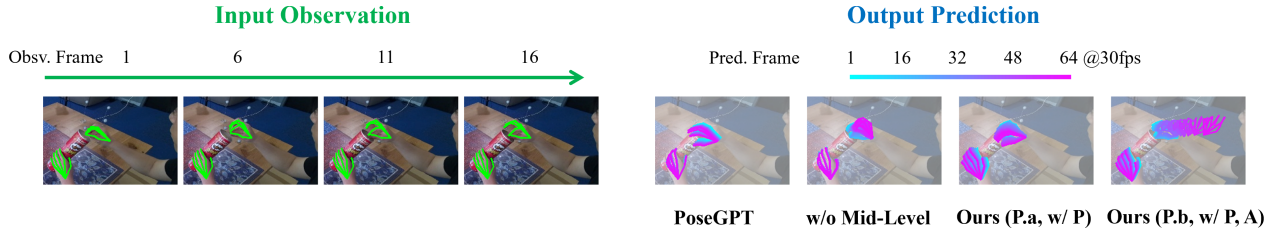


Figure 4. Qualitative comparison of predicted motions for PoseGPT [28], the ablated settings of w/o mid-level, w/ only **P** via path P.a, and the full G-HTT(w/ **P, A**, via path P.b), on H2O [22]. More qualitative cases are provided in the supplementary.

		w/o Mid-Level	w/o Mid-Level	Ours (P.b, w/ P, A)
Sampling with		$\mu, 5\sigma$	$\mu, 10\sigma$	$\mu, 5\sigma$
H2O-Val [22]	FID↓	6.69	14.05	9.30
	APD↑	18.0,23.7	25.5, 33.4	27.8 ,31.4
H2O-Test [22]	FID↓	13.84	22.64	13.10
	APD↑	17.9,29.4	24.1, 35.2	24.6 , 43.3
AssemblyHands Val [35]	FID↓	5.67	6.31	5.21
	APD↑	16.9,21.9	23.3,30.2	33.6 , 40.0

Table 4. Comparison of motion prediction, between ours and the ablated setup without modeling the mid-level, on action sequences that are longer than 2 sec. APD in *mm* for (left,right) hands.

Mid-level for prediction In addition to enabling a decoupled training strategy for **P** and **A** (Sec. 3.4), the modeling of mid-level features should enhance learning of generation. To verify it, we construct a flattened baseline (*i.e.*, w/o mid-level) by removing the mid-level representation and instead using a single transformer VAE to directly model pose and action. In particular, the flattened baseline has its encoder taking hand poses and object as input and producing the action recognition as output, and has its decoder predicting the future hand poses directly. The flattened baseline has comparable amount of parameters as **P** and **A**, and is trained on the same dataset as our framework for fair comparison.

From Tab. 4 we find that under a comparable FID, the mid-level representation enables better diversity (3rd, 5th cols); meanwhile, as we increase the generation diversity of the flattened baseline via more noisy sampling, its accuracy significantly degrades (4th, 5th cols). From Fig. 4, we can see that the flattened baseline results lack global regularity, despite its modeling of pose and action through a powerful end-to-end transformer VAE. The comparison shows that the mid-level representation enables easier learning of global motion regularity, probably because it decouples the complex task of action-guided motion generation into hierarchical subtasks better captured by **P** and **A** respectively.

4.5. Discussion

We make more observations about motion prediction, training strategy and mid-level representation, to give additional understanding of the framework. Due to space limit, we provide more details in supplementary.

Training with Assembly101 [42] We find that including the large-scale Assembly101 for training G-HTT significantly benefits motion prediction on H2O [22] and action

recognition, although it is believed that the pose annotation of Assembly101 is not sufficiently accurate for training pose estimators (*cf.* [35]). The finding points to the importance of large-scale pretraining of fundamental modules.

Predicting action transition We observe that the model can generate smooth transitions between actions (*e.g.* motion depicting *place spray* \rightarrow *apply spray*), although this is never explicitly trained for. It probably comes from training **P** on sequences of mixed action annotations (Sec. 3.4), which allows **P** to drive the transition by decoding local motions into new actions. Meanwhile, it is also facilitated by the decoupled training of **P** and **A**.

The mid-level regularity We blend mid-level features of two different input pose sequences, and decode the blended mid-level features into pose sequences. The generated motions naturally interpolate between the tendencies of two given inputs, showing the regularity of the learned mid-level representation.

5. Conclusion

We present a framework to jointly model both recognition and prediction, and leverage the hierarchy of semantic dependency and temporal granularity, for understanding hand pose and action. The framework addresses tasks of input hand pose refinement, action recognition, and future motion prediction, showing improved performances than isolated solutions. To implement the hierarchy, we cascade two transformer VAE blocks, each modeling pose and action respectively, and introduce a mid-level clip-wise motion representation to bridge the two blocks. Each of the pose and action blocks has its encoder and decoder respectively outputting for the recognition and prediction tasks, while the connected cascade enables regular action and motion modeling over both short and long time spans. We train the two blocks separately to flexibly use multiple datasets with different setups and annotation qualities. Extensive tests validate the performance and design of our framework on both recognition and prediction across different datasets.

Limitations and future work We assume a fixed camera viewpoint for input videos; to process cases with drastic

camera movement (e.g., egocentric views with large head motions), an explicit decomposition of hand and camera motion would be necessary, which we leave as future work. Another aspect is to leverage hand motion as priors for robust recognition of manipulated objects, therefore further benefiting action understanding.

References

- [1] Sadegh Aliakbarian, Fatemeh Sadat Saleh, Mathieu Salzmann, Lars Petersson, and Stephen Gould. A stochastic conditioning scheme for diverse human motion prediction. In *Proceedings of the IEEE/CVF Conference on Computer Vision and Pattern Recognition*, pages 5223–5232, 2020. 2
- [2] Wentao Bao, Lele Chen, Libing Zeng, Zhong Li, Yi Xu, Junsong Yuan, and Yu Kong. Uncertainty-aware state space transformer for egocentric 3d hand trajectory forecasting. *arXiv preprint arXiv:2307.08243*, 2023. 1, 2
- [3] Yujun Cai, Lihao Ge, Jun Liu, Jianfei Cai, Tat-Jen Cham, Junsong Yuan, and Nadia Magnenat Thalmann. Exploiting spatial-temporal relationships for 3d pose estimation via graph convolutional networks. In *Proceedings of the IEEE/CVF international conference on computer vision*, pages 2272–2281, 2019. 2
- [4] Yujun Cai, Yiwei Wang, Yiheng Zhu, Tat-Jen Cham, Jianfei Cai, Junsong Yuan, Jun Liu, Chuanxia Zheng, Sijie Yan, Henghui Ding, et al. A unified 3d human motion synthesis model via conditional variational auto-encoder. In *Proceedings of the IEEE/CVF International Conference on Computer Vision*, pages 11645–11655, 2021. 2, 3
- [5] Joao Carreira and Andrew Zisserman. Quo vadis, action recognition? a new model and the kinetics dataset. In *proceedings of the IEEE Conference on Computer Vision and Pattern Recognition*, pages 6299–6308, 2017. 2
- [6] Mehdi Cherti, Romain Beaumont, Ross Wightman, Mitchell Wortsman, Gabriel Ilharco, Cade Gordon, Christoph Schuhmann, Ludwig Schmidt, and Jenia Jitsev. Reproducible scaling laws for contrastive language-image learning. In *Proceedings of the IEEE/CVF Conference on Computer Vision and Pattern Recognition*, pages 2818–2829, 2023. 4, 5
- [7] Desmond Chik, Jochen Trunpf, and Nicol N Schraudolph. Using an adaptive var model for motion prediction in 3d hand tracking. In *2008 8th IEEE International Conference on Automatic Face & Gesture Recognition*, pages 1–8. IEEE, 2008. 2
- [8] Hoseong Cho, Chanwoo Kim, Jihyeon Kim, Seongyeong Lee, Elkhan Ismayilzada, and Seungryul Baek. Transformer-based unified recognition of two hands manipulating objects. In *Proceedings of the IEEE/CVF Conference on Computer Vision and Pattern Recognition*, pages 4769–4778, 2023. 2
- [9] Eadom Dessalene, Chinmaya Devaraj, Michael Maynard, Cornelia Fermuller, and Yiannis Aloimonos. Forecasting action through contact representations from first person video. *IEEE Transactions on Pattern Analysis and Machine Intelligence*, 2021. 2
- [10] Zhipeng Fan, Jun Liu, and Yao Wang. Adaptive computationally efficient network for monocular 3d hand pose estimation. In *European Conference on Computer Vision*, pages 127–144. Springer, 2020. 2
- [11] Christoph Feichtenhofer. X3d: Expanding architectures for efficient video recognition. In *Proceedings of the IEEE/CVF Conference on Computer Vision and Pattern Recognition*, pages 203–213, 2020. 2
- [12] Christoph Feichtenhofer, Axel Pinz, and Andrew Zisserman. Convolutional two-stream network fusion for video action recognition. In *Proceedings of the IEEE conference on computer vision and pattern recognition*, pages 1933–1941, 2016.
- [13] Christoph Feichtenhofer, Haoqi Fan, Jitendra Malik, and Kaiming He. Slowfast networks for video recognition. In *Proceedings of the IEEE/CVF international conference on computer vision*, pages 6202–6211, 2019. 1, 2
- [14] Chuan Guo, Xinxin Zuo, Sen Wang, Shihao Zou, Qingyao Sun, Annan Deng, Minglun Gong, and Li Cheng. Action2motion: Conditioned generation of 3d human motions. In *Proceedings of the 28th ACM International Conference on Multimedia*, pages 2021–2029, 2020. 2
- [15] Shangchen Han, Beibei Liu, Randi Cabezas, Christopher D Twigg, Peizhao Zhang, Jeff Petkau, Tsz-Ho Yu, Chun-Jung Tai, Muzaffer Akbay, Zheng Wang, et al. Megatrack: monochrome egocentric articulated hand-tracking for virtual reality. *ACM Transactions on Graphics (ToG)*, 39(4):87–1, 2020. 2
- [16] Shangchen Han, Po-chen Wu, Yubo Zhang, Beibei Liu, Linguang Zhang, Zheng Wang, Weiguang Si, Peizhao Zhang, Yujun Cai, Tomas Hodan, et al. Umetrack: Unified multi-view end-to-end hand tracking for vr. In *SIGGRAPH Asia 2022 Conference Papers*, pages 1–9, 2022. 2, 6
- [17] Kaiming He, Xiangyu Zhang, Shaoqing Ren, and Jian Sun. Deep residual learning for image recognition. In *Proceedings of the IEEE conference on computer vision and pattern recognition*, pages 770–778, 2016. 5
- [18] Martin Heusel, Hubert Ramsauer, Thomas Unterthiner, Bernhard Nessler, and Sepp Hochreiter. Gans trained by a two time-scale update rule converge to a local nash equilibrium. In *Advances in Neural*

- Information Processing Systems*. Curran Associates, Inc., 2017. 6
- [19] Umar Iqbal, Pavlo Molchanov, Thomas Breuel Juer-gen Gall, and Jan Kautz. Hand pose estimation via latent 2.5 d heatmap regression. In *Proceedings of the European Conference on Computer Vision (ECCV)*, pages 118–134, 2018. 2
- [20] Biao Jiang, Xin Chen, Wen Liu, Jingyi Yu, Gang Yu, and Tao Chen. Motiongpt: Human motion as a foreign language. *arXiv preprint arXiv:2306.14795*, 2023. 2, 3
- [21] Diederik P Kingma and Max Welling. Auto-encoding variational bayes. *arXiv preprint arXiv:1312.6114*, 2013. 3
- [22] Taein Kwon, Bugra Tekin, Jan Stühmer, Federica Bogo, and Marc Pollefeys. H2o: Two hands manipulating objects for first person interaction recognition. In *Proceedings of the IEEE/CVF International Conference on Computer Vision*, pages 10138–10148, 2021. 2, 6, 7, 8
- [23] Mengcheng Li, Liang An, Hongwen Zhang, Lianpeng Wu, Feng Chen, Tao Yu, and Yebin Liu. Interacting attention graph for single image two-hand reconstruction. In *Proceedings of the IEEE/CVF Conference on Computer Vision and Pattern Recognition*, pages 2761–2770, 2022. 2
- [24] Yin Li, Zhefan Ye, and James M Rehg. Delving into egocentric actions. In *Proceedings of the IEEE conference on computer vision and pattern recognition*, pages 287–295, 2015. 2
- [25] Miao Liu, Siyu Tang, Yin Li, and James M Rehg. Forecasting human-object interaction: joint prediction of motor attention and actions in first person video. In *Computer Vision–ECCV 2020: 16th European Conference, Glasgow, UK, August 23–28, 2020, Proceedings, Part I 16*, pages 704–721. Springer, 2020. 1, 2
- [26] Shaowei Liu, Subarna Tripathi, Somdeb Majumdar, and Xiaolong Wang. Joint hand motion and interaction hotspots prediction from egocentric videos. In *Proceedings of the IEEE/CVF Conference on Computer Vision and Pattern Recognition*, pages 3282–3292, 2022. 1, 2
- [27] Ilya Loshchilov and Frank Hutter. Decoupled weight decay regularization. *arXiv preprint arXiv:1711.05101*, 2017. 5
- [28] Thomas Lucas, Fabien Baradel, Philippe Weinzaepfel, and Grégory Rogez. Posegpt: Quantization-based 3d human motion generation and forecasting. In *European Conference on Computer Vision*, pages 417–435. Springer, 2022. 1, 2, 3, 6, 7, 8
- [29] Ren C Luo and Licong Mai. Human intention inference and on-line human hand motion prediction for human-robot collaboration. In *2019 IEEE/RSJ International Conference on Intelligent Robots and Systems (IROS)*, pages 5958–5964. IEEE, 2019. 2
- [30] Hengbo Ma, Jiachen Li, Ramtin Hosseini, Masayoshi Tomizuka, and Chiho Choi. Multi-objective diverse human motion prediction with knowledge distillation. In *Proceedings of the IEEE/CVF Conference on Computer Vision and Pattern Recognition*, pages 8161–8171, 2022. 2
- [31] Minghuang Ma, Haoqi Fan, and Kris M Kitani. Going deeper into first-person activity recognition. In *Proceedings of the IEEE Conference on Computer Vision and Pattern Recognition*, pages 1894–1903, 2016. 2
- [32] Wei Mao, Miaomiao Liu, and Mathieu Salzmann. Weakly-supervised action transition learning for stochastic human motion prediction. In *Proceedings of the IEEE/CVF Conference on Computer Vision and Pattern Recognition*, pages 8151–8160, 2022. 2, 3
- [33] Gyeongsik Moon. Bringing inputs to shared domains for 3d interacting hands recovery in the wild. In *Proceedings of the IEEE/CVF Conference on Computer Vision and Pattern Recognition*, pages 17028–17037, 2023. 2
- [34] Franziska Mueller, Florian Bernard, Oleksandr Sotnychenko, Dushyant Mehta, Srinath Sridhar, Dan Casas, and Christian Theobalt. Gnerated hands for real-time 3d hand tracking from monocular rgb. In *Proceedings of the IEEE Conference on Computer Vision and Pattern Recognition*, pages 49–59, 2018. 2
- [35] Takehiko Ohkawa, Kun He, Fadime Sener, Tomas Hodan, Luan Tran, and Cem Keskin. AssemblyHands: towards egocentric activity understanding via 3d hand pose estimation. In *Proceedings of the IEEE/CVF Conference on Computer Vision and Pattern Recognition (CVPR)*, pages 12999–13008, 2023. 2, 6, 7, 8
- [36] Mathis Petrovich, Michael J Black, and Gül Varol. Action-conditioned 3d human motion synthesis with transformer vae. In *Proceedings of the IEEE/CVF International Conference on Computer Vision*, pages 10985–10995, 2021. 1, 2, 3
- [37] Mathis Petrovich, Michael J. Black, and Gül Varol. TEMOS: Generating diverse human motions from textual descriptions. In *European Conference on Computer Vision (ECCV)*, 2022. 1, 2, 3
- [38] Alec Radford, Jong Wook Kim, Chris Hallacy, A. Ramesh, Gabriel Goh, Sandhini Agarwal, Girish Sastry, Amanda Askell, Pamela Mishkin, Jack Clark, Gretchen Krueger, and Ilya Sutskever. Learning transferable visual models from natural language supervision. In *ICML*, 2021. 4, 5
- [39] Davis Rempe, Tolga Birdal, Aaron Hertzmann, Jimei Yang, Srinath Sridhar, and Leonidas J Guibas. Humor: 3d human motion model for robust pose estimation.

- In *Proceedings of the IEEE/CVF international conference on computer vision*, pages 11488–11499, 2021. [1](#), [3](#)
- [40] Javier Romero, Dimitrios Tzionas, and Michael J. Black. Embodied hands: Modeling and capturing hands and bodies together. *ACM Transactions on Graphics, (Proc. SIGGRAPH Asia)*, 36(6), 2017. [3](#)
- [41] Christoph Schuhmann, Romain Beaumont, Richard Vencu, Cade W Gordon, Ross Wightman, Mehdi Cherti, Theo Coombes, Aarush Katta, Clayton Mullis, Mitchell Wortsman, Patrick Schramowski, Srivatsa R Kundurthy, Katherine Crowson, Ludwig Schmidt, Robert Kaczmarczyk, and Jenia Jitsev. LAION-5b: An open large-scale dataset for training next generation image-text models. In *Thirty-sixth Conference on Neural Information Processing Systems Datasets and Benchmarks Track*, 2022. [4](#), [5](#)
- [42] Fadime Sener, Dibyadip Chatterjee, Daniel Sheleпов, Kun He, Dipika Singhania, Robert Wang, and Angela Yao. Assembly101: A large-scale multi-view video dataset for understanding procedural activities. In *Proceedings of the IEEE/CVF Conference on Computer Vision and Pattern Recognition*, pages 21096–21106, 2022. [2](#), [6](#), [7](#), [8](#)
- [43] Lei Shi, Yifan Zhang, Jian Cheng, and Hanqing Lu. Two-stream adaptive graph convolutional networks for skeleton-based action recognition. In *Proceedings of the IEEE/CVF conference on computer vision and pattern recognition*, pages 12026–12035, 2019. [1](#), [2](#)
- [44] Mingyi Shi, Sebastian Starke, Yuting Ye, Taku Komura, and Jungdam Won. Phasemp: Robust 3d pose estimation via phase-conditioned human motion prior. In *Proceedings of the IEEE/CVF International Conference on Computer Vision*, pages 14725–14737, 2023. [1](#), [3](#)
- [45] Suriya Singh, Chetan Arora, and CV Jawahar. First person action recognition using deep learned descriptors. In *Proceedings of the IEEE conference on computer vision and pattern recognition*, pages 2620–2628, 2016. [2](#)
- [46] Adrian Spurr, Umar Iqbal, Pavlo Molchanov, Otmar Hilliges, and Jan Kautz. Weakly supervised 3d hand pose estimation via biomechanical constraints. In *European Conference on Computer Vision*, pages 211–228. Springer, 2020. [2](#)
- [47] Bugra Tekin, Federica Bogo, and Marc Pollefeys. H+o: Unified egocentric recognition of 3d hand-object poses and interactions. In *Proceedings of the IEEE/CVF conference on computer vision and pattern recognition*, pages 4511–4520, 2019. [2](#)
- [48] Guy Tevet, Brian Gordon, Amir Hertz, Amit H Bermano, and Daniel Cohen-Or. Motionclip: Exposing human motion generation to clip space. In *European Conference on Computer Vision*, pages 358–374. Springer, 2022. [1](#), [2](#), [3](#)
- [49] Guy Tevet, Sigal Raab, Brian Gordon, Yonatan Shafir, Daniel Cohen-Or, and Amit H Bermano. Human motion diffusion model. *arXiv preprint arXiv:2209.14916*, 2022. [2](#), [3](#)
- [50] Garvita Tiwari, Dimitrije Antić, Jan Eric Lenssen, Nikolaos Sarafianos, Tony Tung, and Gerard Pons-Moll. Pose-ndf: Modeling human pose manifolds with neural distance fields. In *European Conference on Computer Vision*, pages 572–589. Springer, 2022. [3](#)
- [51] Jiayi Wang, Franziska Mueller, Florian Bernard, Suzanne Sorli, Oleksandr Sotnychenko, Neng Qian, Miguel A Otaduy, Dan Casas, and Christian Theobalt. Rgb2hands: real-time tracking of 3d hand interactions from monocular rgb video. *ACM Transactions on Graphics (ToG)*, 39(6):1–16, 2020. [2](#)
- [52] Yilin Wen, Hao Pan, Lei Yang, Jia Pan, Taku Komura, and Wenping Wang. Hierarchical temporal transformer for 3d hand pose estimation and action recognition from egocentric rgb videos. *Proceedings of the IEEE/CVF Conference on Computer Vision and Pattern Recognition*, 2023. [1](#), [2](#), [3](#), [6](#), [7](#)
- [53] Siyuan Yang, Jun Liu, Shijian Lu, Meng Hwa Er, and Alex C Kot. Collaborative learning of gesture recognition and 3d hand pose estimation with multi-order feature analysis. In *European Conference on Computer Vision*, pages 769–786. Springer, 2020. [1](#), [2](#)
- [54] Zhengdi Yu, Shaoli Huang, Chen Fang, Toby P Breckon, and Jue Wang. Acr: Attention collaboration-based regressor for arbitrary two-hand reconstruction. In *Proceedings of the IEEE/CVF Conference on Computer Vision and Pattern Recognition*, pages 12955–12964, 2023. [2](#)
- [55] Ye Yuan and Kris Kitani. Dlow: Diversifying latent flows for diverse human motion prediction. In *Computer Vision—ECCV 2020: 16th European Conference, Glasgow, UK, August 23–28, 2020, Proceedings, Part IX 16*, pages 346–364. Springer, 2020. [2](#), [6](#)
- [56] Yaqi Zhang, Di Huang, Bin Liu, Shixiang Tang, Yan Lu, Lu Chen, Lei Bai, Qi Chu, Nenghai Yu, and Wanli Ouyang. Motiongpt: Finetuned llms are general-purpose motion generators. *arXiv preprint arXiv:2306.10900*, 2023. [2](#), [3](#)
- [57] Yi Zhou, Connelly Barnes, Jingwan Lu, Jimei Yang, and Hao Li. On the continuity of rotation representations in neural networks. In *Proceedings of the IEEE/CVF Conference on Computer Vision and Pattern Recognition*, pages 5745–5753, 2019. [3](#)
- [58] Christian Zimmermann and Thomas Brox. Learning to estimate 3d hand pose from single rgb images. In

*Proceedings of the IEEE international conference on
computer vision*, pages 4903–4911, 2017. [2](#)